Time domain circuit representation of photoconductive gaps in antennas for pulsed terahertz time domain systems

Bernardis, Arturo Fiorellini; Sberna, Paolo; Neto, Andrea; Llombart, Nuria

DOI
10.1109/IRMMW-THz.2019.8874557

Publication date
2019

Published in
IRMMW-THz 2019 - 44th International Conference on Infrared, Millimeter, and Terahertz Waves

Time Domain Circuit Representation of Photoconductive Gaps in Antennas for Pulsed Terahertz Time Domain Systems

Arturo Fiorellini Bernardis[1], Paolo Sberna[1], Andrea Neto[1], Nuria Llombart[1]
[1] Delft University of Technology, EEMCS, The Netherlands

***Abstract*— Pulsed terahertz time-domain systems rely on antennas printed on photoconductive substrates (PCA), which show extremely fast conductivity transients when illuminated by femto-seconds laser pulses. This work introduces a time domain representation of the PCA transmitter that accounts for time evolving voltages at the terminals of the photoconductive gap; such model is able to explain the saturation phenomena observed in measurements performed under high power laser excitations that previous models could not account for.**

I. INTRODUCTION

Photoconductive antennas are able to radiate fields characterized by spectral components up to the THz frequencies. Since they often suffer from low radiated power, accurate detection schemes require long integration times, rendering such architectures adobtable only for short-range niche applications (*e.g.* spectroscopy, testing). Recently, a frequency domain Norton equivalent circuit model developed to aid the design and analysis of such devices was introduced in [1], and the agreement between the results obtained using this model and the relative measurements was validated for low illumination power levels [2], resulting in roughly $110\,\mu W$ of THz radiated power. A much more powerful source, the photoconductive connected array (PCCA) in [3], was then manufactured and measured, reaching $0.7\,mW$ of THz radiated power. However, when the adopted photoconductive substrate (*LT GaAs*) was excited by high levels of laser power, the measurements showed saturation phenomena that the Norton circuit could not explain. The equivalent circuit in [1] models a time bias voltage, V_B, on the gap that remains constant, while the induced conductance value, $g(t, P_L, \mu, w_{gap})$, changes with time. This conductance is function of the incident optical power P_L, the carrier mobility μ, and the gap dimension w_{gap}. The current generator of the Norton circuit model is expressed in the time domain as the product between the voltage over the gap and the induced photoconductance:

$$i_g^{(I)} = V_B g(t, P_L, \mu, w_{gap}) \tag{1}$$

Using this current generator, a Norton impedance consisting in the average of $g(t)^{-1}$ over an interval $t_{on} = 1.5ps$, and an antenna radiation resistance of $R_a = 70\Omega$, the radiated power results quadratically proportional to the incident laser power. After having considered possible reasons (Joule heating, carriers saturation, different mobility etc.), to address the radiated power saturation issue, with this work we propose a novel electrical model that accounts for decreasing voltages across the gap terminals, $v_g(t) \neq V_B$.

II. GAP VOLTAGE DISCHARGE

A PCA consists of a metallization printed over a slab of photoconductive material, namely low temperature grown *(LT) GaAs*, connected to the bias lines and radiating into a hemispherical Si lens. The structure is then periodically excited by a femto-seconds laser that injects carriers in the conduction band of the substrate giving rise to extremely fast conductivity transient. Effectively, the metallization and the photoconductive gap represent a capacitance, and together with the conductance transient induced by the pulsed laser, $g(t)$, can be represented as a switched RC circuit. This configuration is charged by the bias lines when no laser is present ($g(t) \to \infty$), while discharged when the laser is present, as $g(t)$ reaches significantly high values; indeed, under the assumption that the biasing circuitry is not able to react in the $t_{on} = 1.5\,ps$ time-span of the conductivity transient, large quantities of free carriers get injected in the conduction band by the optical excitation, creating a short-circuit over the gap. The conductivity transient induced by the incoming optical excitation is expressed as the convolution between the laser Gaussian time envelope, $l(t)$, and the material impulse response, $h(t)$, as $g(t) = l(t) * h(t)$. Consequently, the evolution of the voltage across the antenna gap is given by the following expression:

$$v_g(t) = \begin{cases} V_B & t < 0 \\ V_B e^{-\int_0^t \frac{g(\tau)}{C_g} d\tau} & t \geq 0 \end{cases} \tag{2}$$

Where the signal evolution after the laser pulse arrives, $t > 0$, can be seen as a RC discharge with a varying time constant $\tau_{RC}(t) = C_g / g(t)$.

Attention must be paid to the fact that the capacitance that contributes to the aforementioned discharge, C_g, is not the DC capacitance introduced by the biased metallization. As a matter of fact, t_{on} is so short that only some of the carriers accumulated on the metals contribute to the current signal crossing the gap, and the capacitance we refer to is representative only of them. Moreover, this capacitance shows a dependency on the bias level: the greater the bias voltage, V_B, the greater the density of accumulated carriers, and the higher the contribution to the gap-current that will excite the antenna.

III. RESULTS

The parameters of the adopted materials are: carrier recombination time constant, $\tau_r = 0.3\,ps$; carrier mobility, $\mu = 400 cm^2/V/s$; absorption coefficient, $\alpha = 1\,\mu m$; reflection coefficient, $\Gamma = 0.5477$; energy band gap frequency, $f_c = 375\,THz$. The laser has a Gaussian time envelope of duration, $\tau_L = 0.1\,ps$. The gap is a square of side, $w_{gap} = 10\,\mu m$, and height, $w_z = 2\,\mu m$. Fig 1 shows

the discussed discharge for a bias voltage of $V_B = 40V$, along with the normalized time envelope of the induced conductivity transient, for three different laser power levels, $P_L = 10, 30, 50\ mW$. It is interesting to note that in case of lower and lower power levels the discharge tends not to be complete, bringing the model proposed in this manuscript closer and closer to the one introduced in [1]. The current signal flowing in the gap is given by:

$$i_g^{(II)} = v_g(t)g(t, P_L, \mu, w_{gap}) \tag{3}$$

This current is different with respect to what used for the model in [1], and can explain the saturation phenomena observed in the measurements in [3]. Indeed, as emerging from Fig. 1, the discharge induced at the antenna terminals becomes less negligible as the optical power increases, and the generated signal, $i_g^{(II)}$, that otherwise would follow the conductance temporal evolution, as in (1), is choked by the rapidly decreasing voltage given by (2). In other words, this phenomenon affects the slower decaying tail of the conductance, effectively decreasing the energy of the low frequency portion of the spectrum of $i_g^{(II)}$.

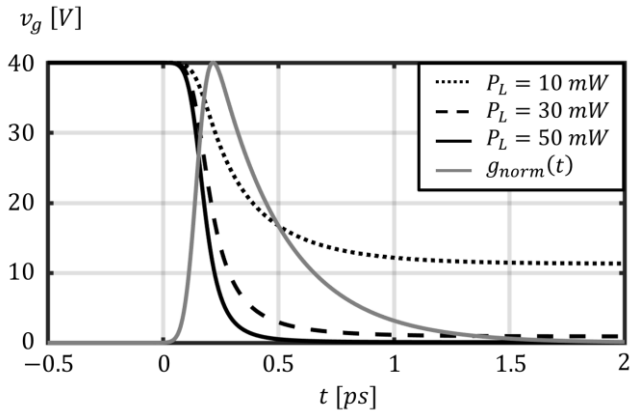

Fig.1: Discharge at the antenna terminals under the presence of the incoming laser pulse for three different optical powers, $P_L = 10, 30, 50\ mW$. The grey solid line shows the normalized time envelope of the induced photoconductivity.

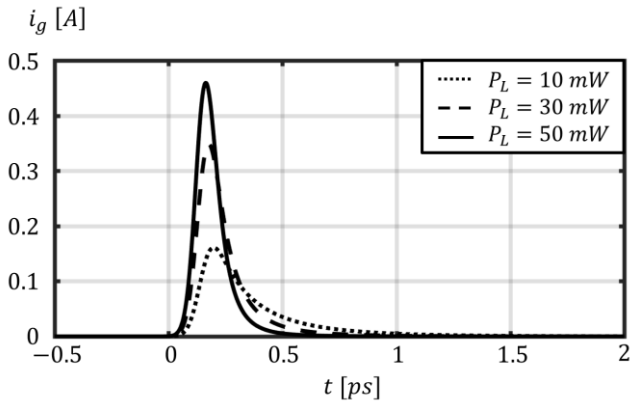

Fig.2: current signal induced across the gap estimated using the proposed model, $i_g^{(II)}$, for three different laser illumination levels, $P_L = 10, 30, 50\ mW$.

Fig (3) shows the comparison of the results predicted by the voltage discharge model proposed in this manuscript with the measurements taken with a bow-tie photoconductive antenna with a gap $w_{gap} = 10\ \mu m$. The parameters are those mentioned at the beginning of the section, and radiated power is calculated and measured as a function of the incident laser power, for different biasing levels and for different C_g values, according to what explained in section II; the bow-tie radiation resistance is $R_a = 70\ \Omega$, constant over the bandwidth of interest. It is apparent that this novel model predicts a radiated power that follows the saturation effects emerging from the measurements under high laser power excitations.

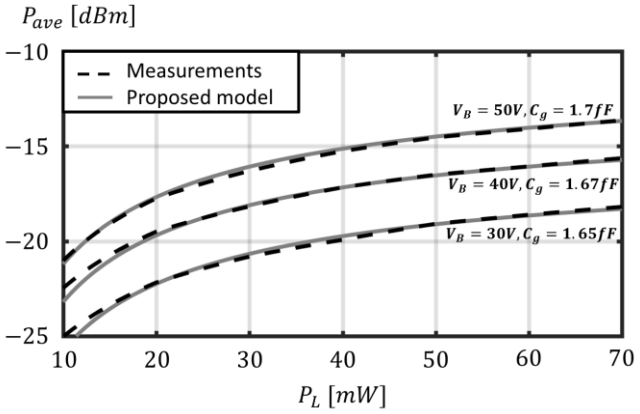

Fig.3: radiated power as a function of the incident optical power estimated by the present voltage discharge model and compared to the measurements taken for a bow-tie with gap $w_{gap} = 10\ \mu m$. Three different bias voltages accounted for: $V_B = 30, 40, 50\ V$.

For the sake of clarity, Fig.4 shows the radiated power estimated by the model presented in [1], along with the results of Fig. 3, for one single biasing level, $V_B = 40V$.

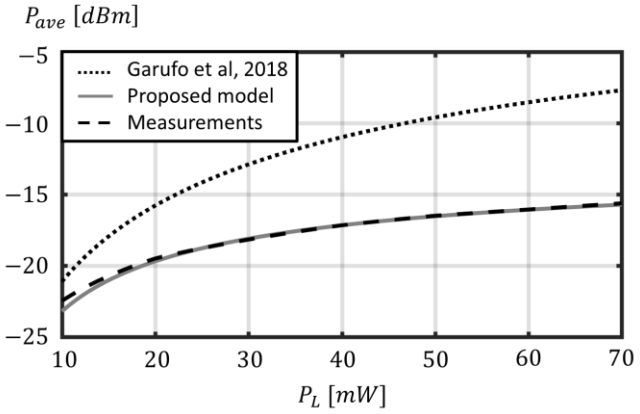

Fig.4: comparison of the radiated power as a function of the incident optical power estimated by the present voltage discharge model, by the Norton equivalent circuit in [1] and compared to the measurements taken for a bow-tie with gap $w_{gap} = 10\ \mu m$, for a bias level of $V_B = 50\ V$.

REFERENCES

[1] A. Garufo, G. Carluccio, N. Llombart and a. Neto, "Norton Equivalent Circuit for Pulsed Photoconductive Antennas–Part I: Theoretical Model", *IEEE Trans. Antennas Propag.*, vol. 66, no. 4, 2018.

[2] A. Garufo, G. Carluccio, J. R. Freeman, D. R. Bacon, N. Llombart, E. H. Linfield, A. G. Davies and A. Neto, "Norton Equivalent Circuit for Pulsed Photoconductive Antennas—Part II: Experimental Validation", *IEEE Trans. Antennas Propag.*, vol. 66, no. 4, 2018.

[3] A. Garufo; P. Sberna; G. Carluccio; J. Freeman; D. Bacon; L. Li; J. Bueno; J. Baselmans; E. Linfield; A. Davies ; N. Llombart; A. Neto. "A Connected Array of Coherent Photoconductive Pulsed Sources to Generate mW Average Power in the Submillimeter Wavelength Band", *IEEE Trans. THz Sci. Technol.*, early access, 2019